

## PRECIPITATION GROWTH MECHANISMS IN A BAY OF BENGAL DEPRESSION

Robert A. Houze, Jr., and Dean D. Churchill

Department of Atmospheric Sciences  
University of Washington  
Seattle, WA 98195

### 1. Introduction

During the Summer Monsoon Experiment of the Global Atmospheric Research Programme (Summer MONEX), the National Oceanic and Atmospheric Administration's WP3D research aircraft (the P3) the National Center for Atmospheric Research Electra aircraft were used in a detailed investigation of a depression located over the Bay of Bengal during 3-8 July 1979. Depressions of this type move westward and account for the bulk of the mid-summer monsoon rain over northern and central India. The aircraft investigation of the Summer MONEX depression was unique among studies of the Asian Monsoon. On no other occasion has such advanced instrumentation been used to observe these important storms. This paper describes the mechanisms of precipitation growth in the depression revealed by the quantitative radar and cloud microphysical probes aboard the P3 during this unique experiment.

### 2. Mesoscale structure of the clouds and precipitation

The airborne radar data showed that the precipitation in the depression was located in mesoscale precipitation features. These features were typically 100-300 km in horizontal dimension and were located northwest through southwest through southeast of the storm center. Each mesoscale precipitation feature was characterized by a widespread cloud shield based at about the 400 mb level (Warner and Grumm, 1984). The rain falling from the cloud deck resembled that in equatorial cloud clusters in that it was partly convective and partly stratiform. (For discussions of cloud clusters, see Houze and Betts, 1981; Houze et al., 1981; Churchill and Houze, 1984). The convective portion contained vigorous cloud towers, which overshoot the tops of the cloud shields of the mesoscale precipitation features and produced narrow cores and lines of intense precipitation. However, the stratiform region, which consisted of relatively uniform moderate rain, usually dominated the area covered by precipitation in each mesoscale feature.

### 3. Precipitation growth mechanisms

The stratiform regions of the mesoscale precipitation features in the depression were traversed extensively by the P3 aircraft at flight levels ranging in temperature from +5 to -25°C. Hydrometeor images were obtained on these flights with Particle Measuring Systems (PMS) cloud and precipitation probes. The cloud probe detected

hydrometeors up to 1.66 mm in dimension, while the precipitation probe detected particles up to 6 mm in dimension. These data provided a unique view of the precipitation mechanisms at work in the stratiform regions of the mesoscale precipitation features.

Cloud liquid water (detected by the Johnson-Williams hot-wire technique) was virtually absent ( $\leq .1 \text{ g/m}^3$ ) above the 0°C level. Consequently, we infer that the cloud regions penetrated by the P3 aircraft at these altitudes were glaciated, or very nearly so. Our microphysical analysis therefore emphasizes the identification and interpretation of the ice particles encountered along the flight tracks of the aircraft. Because of the wide range of flight altitudes, particle images obtained aboard the P3 were especially suitable for examining the vertical distribution of ice particle types in the deep stratiform clouds of the depression and thereby inferring the types of precipitation growth mechanisms that were operative in those regions.

The P3 aircraft flew through the depression on 3, 5, 6, 7 and 8 July. Data from all of the flights are combined in Table 1, where they are grouped according to flight-level temperature and observed particle type. The data from flight tracks through regions of convective cells (0959-1001 GMT on 3 July, 0353-0354 on 5 July and 1005-1007 on 5 July) have been omitted. For a given temperature range and particle category, we divided the total number of observed particles by the number of minutes that the aircraft was in cloud. The resulting mean concentration, in units of #/min, is indicated in Table 1 for each particle type and temperature range.

The data in Table 1 are presented graphically in Fig. 1. The vertical distributions shown are highly consistent both with each other and with the expected structure of precipitating stratiform clouds. The particle types in Figs. 1a and b have identifiable crystal habits, which are known to nucleate at certain ambient temperatures. If the particles are assumed to have fallen about 1 km from their altitude of nucleation<sup>1</sup> before being sampled by the aircraft, then their nucleation temperature must have been about 6 °C lower than the flight-level temperatures indicated in Fig. 1 and Table 1. For example, a flight-level temperature of -5 °C would correspond to a nucleation temperature ( $T_N$ ) of about -11 °C. The following discussion demonstrates that, under the assumption of this amount of downward

<sup>1</sup>This amount of downward particle displacement would require about 15 min at a fallspeed of 1 m/s.

*Table 1. Hydrometeors of various types detected by Particle Measuring Systems (PMS) 2-D probes aboard the NOAA WP3D aircraft during Summer MONEX flights into the Bay of Bengal depression of 3-8 July 1979. The data are grouped according to flight-level temperature. The total number of minutes of flight in each temperature range are indicated in parentheses. The numbers shown for each type of particle have units of #/min. They are the average numbers of particles encountered per minute of in-cloud flight at the indicated temperature range; that is, for each type of particle, the numbers shown below are A/B, where A is the total number of particles of a given type detected while flying at levels characterized by a given temperature range, and B is the total number of minutes of flight in cloud in that temperature range. The aggregates and large dendritic crystals were identified in data from the PMS precipitation probe. All the other particle types were identified in data from the PMS cloud probe.*

<u>Temperature</u>	<u>Nearly round</u>	<u>Columns</u>	<u>Small Dendritic</u>				<u>Large</u>
			<u>Crystals</u>	<u>Needles</u>	<u>Plates</u>	<u>Aggregates</u>	<u>Dendritic Crystals</u>
-20.1° to -24.0°C (48 min)	1.0	0.4	0.1	0	0	0	0
-16.1° to -20.0°C (117 min)	0.6	4.3	0.6	0.1	0.1	0.5	0.02
-12.1° to -16.0°C (97 min)	0.7	3.4	0.7	0.1	0.1	6.6	0.8
-10.1° to -12.0°C (68 min)	0.9	2.0	1.5	0.3	0.2	11.7	2.3
-4.1 to -10.0°C (65 min)	1.4	1.3	2.0	0.02	0.4	27.3	4.0
0° to -4.0°C (89 min)	3.4	3.0	0.1	8.5	0.03	21.4	0.1
≥ 0.1°C (43 min)	16.1	0.3	0	0.5	0	7.8	0

displacement of the ice particles from their level of origin, the maxima and minima of the curves in Figs. 1a and b occur at the expected temperatures.

The concentration of needles (Fig. 1a) was maximum at a flight-level temperature of -2 °C. According to the above assumption of one kilometer of sedimentation, the particles would have formed at a  $T_N$  of about -8 °C, which is within the temperature regime in which needles are formed.<sup>2</sup> The vertical distribution of columns is characterized by maxima at -2 and -18 °C (or  $T_N = -8$  and -24 °C). These temperatures correspond to the two favored temperature regimes of columnar crystal growth in the atmosphere. These occur at  $T_N = -8$  to -10 °C and  $T_N = -20$  to -28 °C.

Figure 1b displays the vertical distributions of plates, small dendritic crystals and large dendritic crystals. The distributions of plates and small dendritic crystals closely parallel each other. This similarity is reasonable since branched crystals, especially dendrites, stellars, sector plates and the

<sup>2</sup>The temperature and humidity conditions for the growth of natural snow crystals are well known. The nucleation temperatures we refer to in this discussion were obtained from Fig. 10.11 of Hobbs (1974).

like, are actually modified plates. The plates, small dendritic crystals and large dendritic crystals share the same flight-level temperature of maximum concentration (-11 °C). The peak is particularly well marked for the large dendritic crystals. The corresponding nucleation temperature, under the assumption of 1 km of fallout, is  $T_N = -17$  °C, which falls within the primary regime of natural branched crystal growth ( $T_N = -12$  to -17 °C). The maximum of large dendritic crystal concentration is rather broad, extending over flight-level temperatures of about -7 to -12 °C, corresponding to nucleation temperatures  $T_N = -13$  to -18 °C, which fall nearly perfectly within the natural growth regime.

The two maxima for columnar crystals seen in Fig. 1a straddle the level of maximum concentration of plates, small dendritic crystals and large dendritic crystals seen in Fig. 1b. This comparison is consistent with the known tendency for the production of crystals to vary from prismatic at  $T_N = -4$  to -10 °C to platelike at  $T_N = -10$  to -22 °C back to prismatic at  $T_N < -22$  °C (see Table 4.2 of Wallace and Hobbs, 1977). We must be somewhat cautious in this interpretation, however, because the maximum of columns at -2 °C could have resulted from inadvertent misclassification of needles, which were numerous at this level.

In Fig. 1c, we have plotted the distributions of particle types that did not exhibit pristine crystalline habits but rather were recognizable by their images as being either aggregate snowflakes or nearly round particles. The latter were undoubtedly raindrops at flight-level temperatures  $> 0^{\circ}\text{C}$ , where their concentration increased abruptly. Above the melting level, the nearly round particles were either aggregates that produced a nearly round image, or they were rimed particles, possibly graupel. Since the cloud liquid water content observed on these flights was generally negligible, it is unlikely that riming could have been active enough to produce graupel in the stratiform clouds. However, some of the flight tracks passed close to convective cells, which may have contained large enough amounts of liquid water to have produced rimed particles that were subsequently detrained into the stratiform cloud regions traversed by the aircraft.

The concentration of aggregate snowflakes exhibited a pronounced maximum at flight-level temperatures between  $0$  and  $-10^{\circ}\text{C}$  (Fig. 1c). It is significant that this maximum is centered just below the maxima of platelike and dendritic crystals seen in Fig. 1b. This juxtaposition suggests that the large aggregates were formed by the entanglement of large dendritic crystals. This inference is supported by the tendency, noted in the examination of the distribution of particle types along individual flight tracks, for aggregates to be encountered wherever large dendritic crystals occurred profusely.

These results present a rather clear picture of stratiform precipitation mechanisms. Ice crystals were consistently nucleating at temperatures corresponding to their shapes and settling downward as they grew. The downward drift of the ice particles, with terminal fallspeeds of only  $1-2\text{ m/s}$ , could only have occurred in regions of weak upward motion, of the type associated with deep stratiform cloud. Branched crystals were apparently aggregating as they descended toward the  $0^{\circ}\text{C}$  level with the result that aggregates were common in a  $2\text{ km}$  deep layer just above the melting level. Below this level, the aggregates and other ice particles abruptly melted and turned to raindrops.

#### 4. Conclusions

The characteristically stratiform microphysical character of the clouds associated with the mesoscale rain areas of the Bay of Bengal depression emphasizes the importance of the stratiform precipitation growth process in storms of this type. The widespread areas of horizontally uniform, moderate rainfall were nonconvective. This result is significant since these nonconvective portions of the mesoscale rain areas dominated the total area covered by precipitation in the depression. Any view of the clouds and precipitation in the Bay of Bengal depression must take into account this stratiform structure.

The vertical stratification of microphysical mechanisms seen in the results of this study prevailed along  $100-300\text{ km}$  segments of the flight tracks. This result implies that updrafts strong

enough to promote ice particle growth, but not strong enough to prevent sedimentation of the particles or to maintain liquid water in the presence of the ice, must have prevailed above the  $0^{\circ}\text{C}$  level in the stratiform regions of the mesoscale precipitation features in the Bay of Bengal depression. These mesoscale regions of upward motion of intermediate intensity undoubtedly play an important role in the dynamics of the depression along with stronger but less widespread convective-scale vertical motions.

#### Acknowledgements

Dr. Paul Herzegh was the radar and cloud-physics scientist on board the NOAA WP3D aircraft, and he processed the PMS particle images for us. Abhik Biswas and Terri Rottman reduced the microphysical data, and Kay Moore drafted the figures. This research was sponsored by the National Science Foundation, Grant No. ATM-8413546, and the Scientific Computing Division of the National Center for Atmospheric Research.

#### References

- Churchill, D.D., and R.A. Houze, Jr., 1984: Development and structure of winter monsoon cloud clusters on 10 December 1978. J. Atmos. Sci., **41**, 933 - 960.
- Hobbs, P.V., 1974: Ice Physics. Clarendon Press, 803 pp.
- Houze, R.A., and A.K. Betts, 1981: Convection in GATE. Reviews of Geophysics and Space Physics, **19**, 541-576.
- Houze, R.A., Jr., S.G. Geotis, F.D. Marks, Jr., and A.K. West, 1981b: Winter monsoon convection in the vicinity of north Borneo, Part I: Structure and time variation of the clouds and precipitation. Mon. Wea. Rev., **109**, 1595-1614.
- Wallace, J.M., and P.V. Hobbs, 1977: Atmospheric Science: An Introductory Survey. Academic Press, New York, 467 pp.
- Warner, C., and R. H. Grumm, 1984: Cloud distributions in a Bay of Bengal monsoon depression. Mon. Wea. Rev., **112**, 153 - 172.

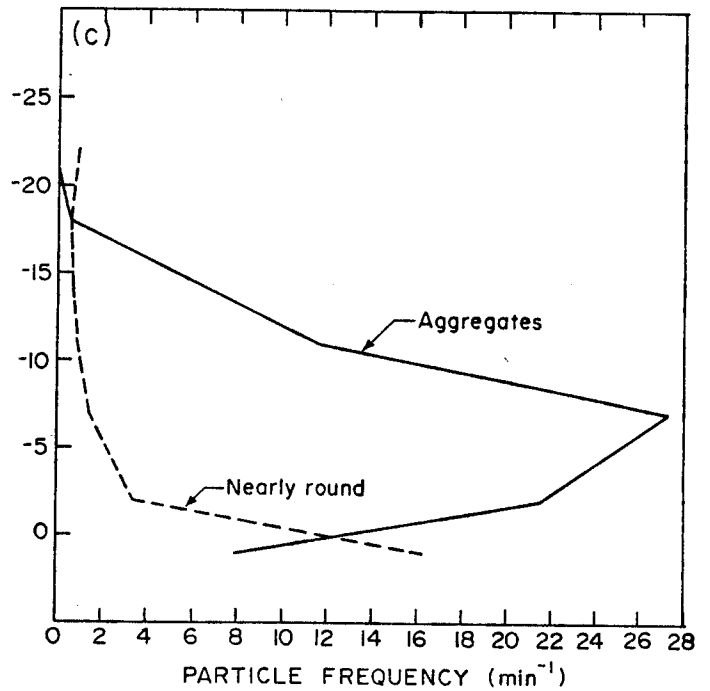
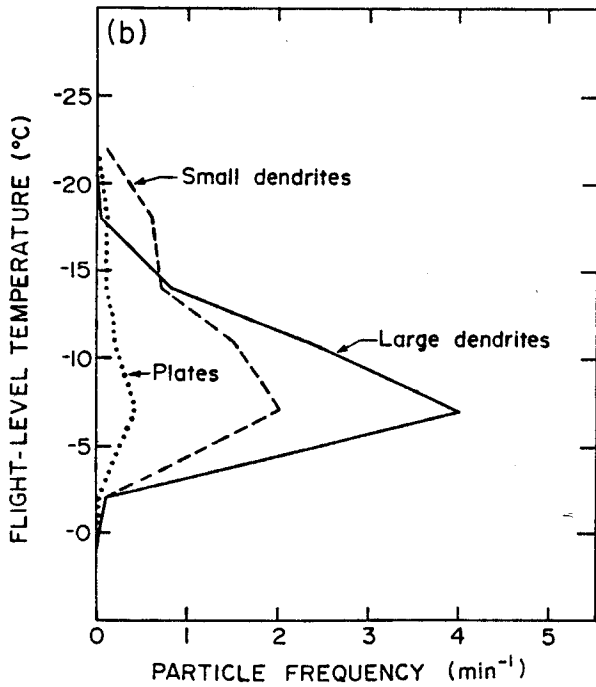
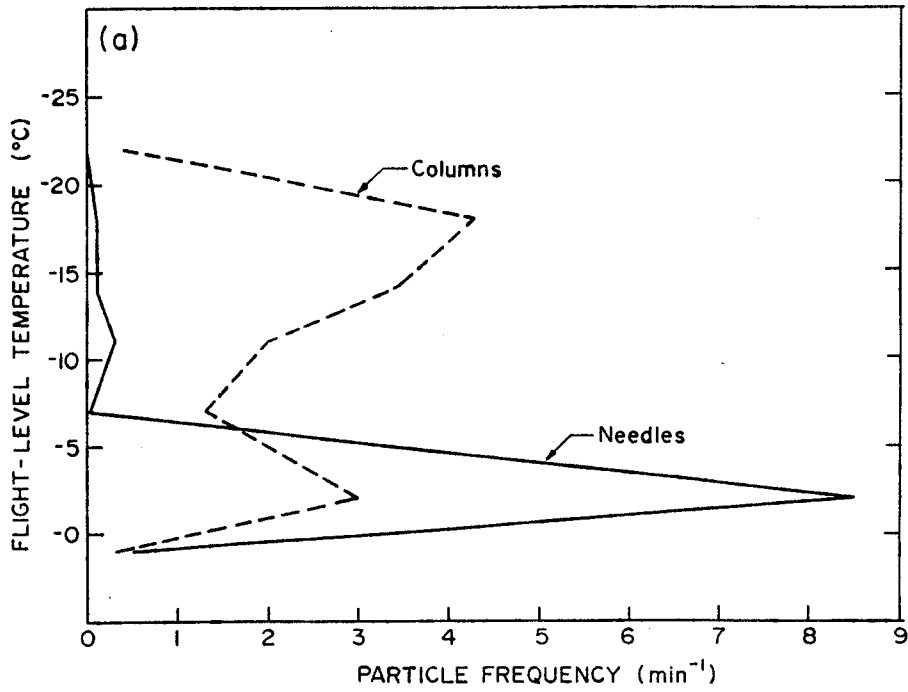


**Figure 1.** Concentrations of particles of various types sampled by the P3 aircraft as functions of flight-level temperature. The information plotted is the same as that in Table 1. Data in (a) and (b) refer to pristine crystal types. Data in (c) refer to particle types that did not exhibit pristine crystalline habits.